Middle East Journal of Applied Sciences
ISSN 2077-4613

Volume : 07 | Issue :03 |July-Sept.| 2017
Pages: 586-594

Easy and Environment-Friendly Synthesis of Graphene by γ- Irradiation

[1]Atta M. M., H. Reheim[1], H. A. Ashry[1] and G. M. Nasr [2] and M. Omar [2]

[1]National Center for Radiation Researches and Technology, Egyptian Atomic Energy Authority, Cairo, Egypt
[2] Physics Department, Faculty of Science, Cairo University, Cairo, Egypt

Received: 20 July 2017 / Accepted: 25 August 2017 / Publication date: 20 Sept. 2017

ABSTRACT

Taking into account the advantages of graphene synthesis by γ-irradiation such as environment -friendly, the absence of toxicity, temperature independent and low cost; the reduction of graphene oxide (GO) by γ-irradiation to obtain graphene has been investigated. Radiation reduced graphene oxide samples (RRGOs) with different reduction degree were obtained by dissolving GO in ethanol/water mixture and directly irradiated by three different doses. Also, chemically reduced graphene oxide sample (CRGO) was prepared for comparison. X-Ray diffraction (XRD), Fourier transforms infrared spectroscopy (FTIR), and Thermogravimetric analysis (TGA) techniques were used to reduction verification. It was found that the reduction degree of RRGOs dependent on the absorbed dose. Also, the electrical conductivity of RRGOs was reliant on irradiation dose and reached comparable value to CRGO. Furthermore, RRGOs have improved thermal stability compared to CRGO in a definite temperature spans.

Key words: Graphene oxide, γ-Irradiation, Graphene, Reduced graphene, Environment

Introduction

Compared to other carbon allotropes, wonderful features of graphene made it one of best promising materials. It's beneficial in various applications such as transparent conductive films (Junbo *et al.,* 2010), Energy storage devices (Xuan *et al.,* 2008), solar cells (Hsu *et al.,* 2012), Li -ion batteries (Donghai *et al.,* 2009) and supercapacitors (Meryl *et al.,* 2008).

Various synthetic methods have been reported for graphene production such as mechanical exfoliation (Yuanbo *et al.,* 2005), epitaxial growth (Walt *et al.,* 2007), and chemical vapor deposition (Alfonso *et al.,* 2009). Though a very high- quality graphene produced from these methods, it's not suitable for large or industrial production.

Reduction of graphene oxide (GO) is a common manner for large scale graphene production. There are numerous reduction methods such as thermal (Dongxing *et al.,* 2009), solvothermal (Hailiang *et al.,* 2009) and electrochemical methods (Yuyan *et al.,* 2010); but the chemical reduction is the most common method for reduction of graphene oxide. All of these methods have many disadvantages such as high temperature required, explosive and toxicity of chemically reducing agents that harmful to the environment as well as high cost needed (Ding *et al.,* 2011; Chen *et al.,* 2011). To solve these problems; recently γ- rays is used to GO reduction (Bowu *et al.,* 2012; Leila *et al.,* 2015). Reduction of GO by γ-irradiation is based on radiolysis of water into oxidative and reductive radicals where GO should be dispersed in aqueous solution (Helen, 1998). To remove oxidative radicals and γ-ray induced reduction, it was reported that oxygen-free (de-oxygenation) and alcohol adding are mandatory. Where alcohol role is scavenging oxidative radicals whereas de-oxygenation is removing dissolved oxygen (Bowu *et al.,* 2012). In another study, reduced graphene oxide was obtained by low absorbed dose rate of a gamma ray. GO was dispersed in the solution of ethanol /water (50:50) and de-oxygenation by nitrogen bubbling was also performed before irradiation (Leila *et al.,* 2015).

The present study investigate a new trial for reduction of GO based on γ-irradiation, without de-oxygenation. In this concern, GO was dispersed in water / ethanol mixture and directly irradiated by three different doses of γ-rays. Also, chemically reduced graphene oxide sample was prepared carefully for comparison studies.

Corresponding Author: Atta M. M., National Center for Radiation Researches and Technology, Egyptian Atomic Energy Authority, Cairo, Egypt. E-mail: mmatta2007@yahoo.com

Experimental

Materials

Graphite fine powder (<50μ m) was purchased from Merk chemicals company, Germany. Hydrazine hydrate was purchased from Sigma-Aldrich Company, USA. Ethanol (96%) was purchased from El Nasr pharmaceutical chemicals company, Egypt.

Preparation of Radiation Reduced Graphene Oxide Samples (RRGOs)

GO was prepared from graphite based on improved Hummer's method discussed somewhere else (Daniela *et al.,* 2010). RRGOs were prepared as follows: 200 mg of GO was dispersed in 200 ml of water /ethanol mixture (50 v/v %) using the ultrasonic bath for 45 min then irradiated at room temperature with γ -rays from a ^{60}Co source. The total absorbed doses were 20, 40 and 80 kGy; the dose rate was 2 kGy h^{-1}. After irradiation, the color of GO dispersion was turned from yellow to black. The obtained product was filtrated, washed and oven-dried overnight.

Preparation of Chemically Reduced GO Sample (CRGO)

CRGO was prepared as follows: GO solution was produced by adding 300 mg of graphene oxide into 100 ml of distilled water under mechanical stirring then 0.3 ml of hydrazine was added to the solution. Then the mixture was heated in an oil bath at 80^{o}C with continuous stirring for 24 h. Finally, the produced CRGO was filtrated, washed and oven-dried overnight.

Characterization techniques

The chemical structure of samples was investigated using Fourier Transform Infrared Spectroscopy FT-IR (Shimadzu Prestige-21 Spectrophotometer) in the 4000-500 cm^{-1} range. X-ray diffraction analysis (XRD) was performed on an X-ray diffractometer (Shimadzu X-Lab) with a Cu-K_α radiation source (λ=1.54Å) in the range of 4–90^{o}, the interlayer distance was calculated based on Bragg's law. Raman spectroscopy was performed by Witec alpha 300 R confocal Raman microscopes with 532 nm laser excitation source. Transmission electron microscopy (TEM) was carried out using a JEOL, JEM-100Cx microscope operated at 120 kV.

The conductivity of compressed powder pellets of samples was measured by Keithley 6514 electrical measurement system. The thermal stability was measured using a Thermogravimetric analyzer (TGA, Shimadzu–50) between ambient temperature and 700˚C at a heating rate of 5˚C min^{-1} under a nitrogen atmosphere.

Results and discussion

Figure (1) shows FTIR spectra for Graphite, GO, CRGO and RRGOs prepared at different doses. There are no observed bands in Graphite while in GO, a strong broad band around 3400 cm^{-1} attributed to the O-H stretching vibrations of water and C-OH groups was observed. Strong bands observed at 1735 and 1620 cm^{-1} corresponding to stretching vibrations of carbonyl C=O and aromatic C=C respectively (Xiangbo *et al.,* 2010). Epoxide C-O stretching vibrations observed at nearly 1210 and 1030 cm^{-1}. These bands refer to a very high content of oxygen functional groups held in GO during oxidation.

For RRGOs, intensities of GO bands were dramatically decreased with an increase in the absorbed dose; indicate removing of oxygen functional groups and efficient reduction of GO by γ-irradiation (Choi *et al.,* 2010). FTIR Spectra of RRGOs at 40, 80 kGy are very similar indicate nearby reduction degree.

The X-Ray diffraction (XRD) technique provides essential information about structural changes in GO during the reduction process. Figure (2) shows XRD for Graphite, GO, CRGO and RRGOs prepared at different doses. A basal reflection (002) Graphite peak at 2θ =26.32° represents stacked

carbon atoms arranged in a honeycomb structure. By oxidation, Graphite peak shifted to a lower angle at 8.5° corresponding to a larger interlayer spacing which ascribed to water and oxygen functional groups held in GO (Buchsteiner *et al.,* 2006).

For RRGOs, sharp peak of GO disappeared with an increase in irradiation dose. Where at 20 kGy, GO peak shifted to 10.6 ° with decreased intensity and two a new peaks appeared at 13.9 and 22.7 ° corresponding to an interlayer spacing 6.35 and 3.9 Å respectively, indicate GO still containing oxygen –functional groups or partially reduced.

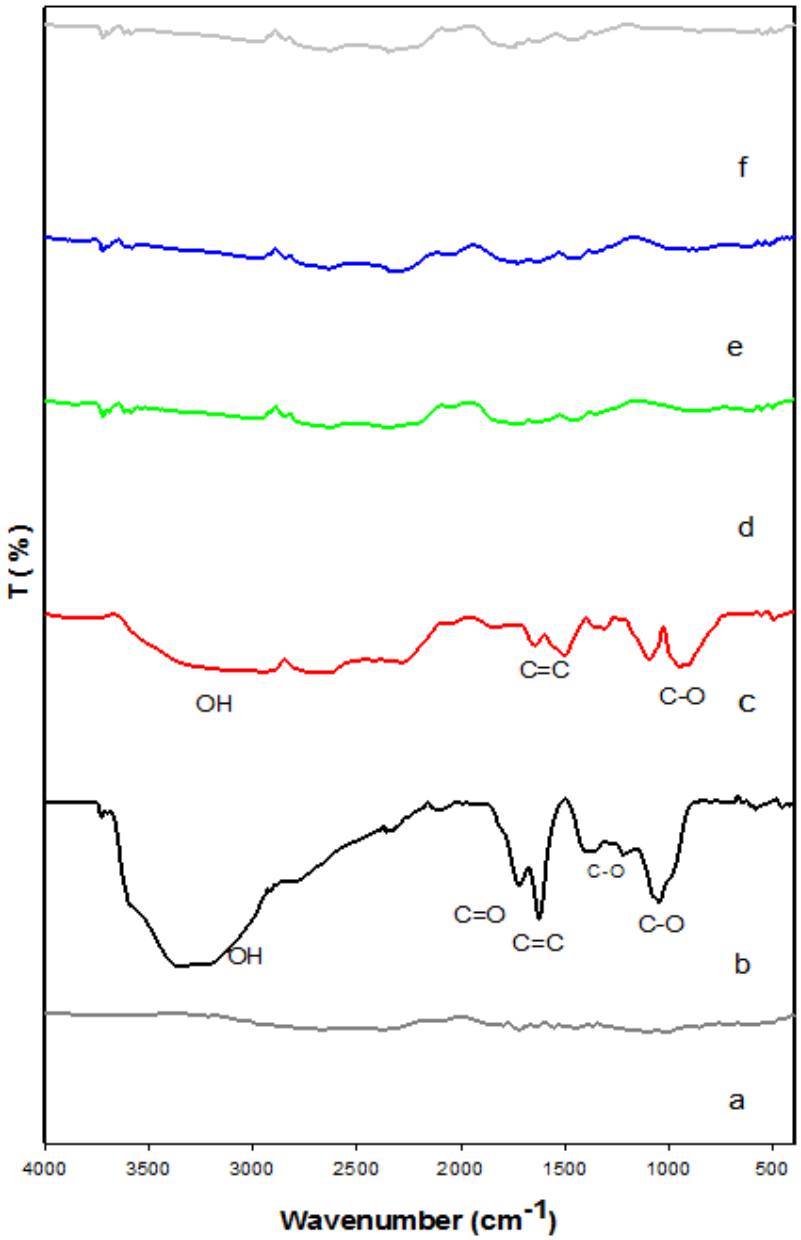

Fig. 1: FTIR spectra for Graphite (a) GO (b) and RRGOs prepared at different absorbed doses of 20 (c) 40(d) and 80 KGy (e) compared to CRGO (f).

Only broad peak at 23° and 23.1° was observed in RRGOs at absorbed doses 40 and 80 kGy, corresponding to interlayer distance of 3.86 and 3.83 Å, respectively. These interlayer distance values are very similar to that of Graphite and CRGO, which indicate elimination of most of oxygen species

by increasing absorbed dose (Bowu *et al.,* 2012) as well as approximate reduction level of RRGO at 40 and 80 kGy. These results were consistent with FTIR data.

The interlayer distance of CRGO is slightly higher than that of the RRGOs at 40 and 80 kGy which indicate few residual oxygen functional groups held in RRGOs and slightly increased reduction degree of CRGO. The small peak at 2θ = 42.3° in RRGOs and CRGO samples corresponding to an interlayer spacing of 2.12 Å, could be due to the turbostratic band of disordered carbon.(Zhiwei *et al.,* 2010).

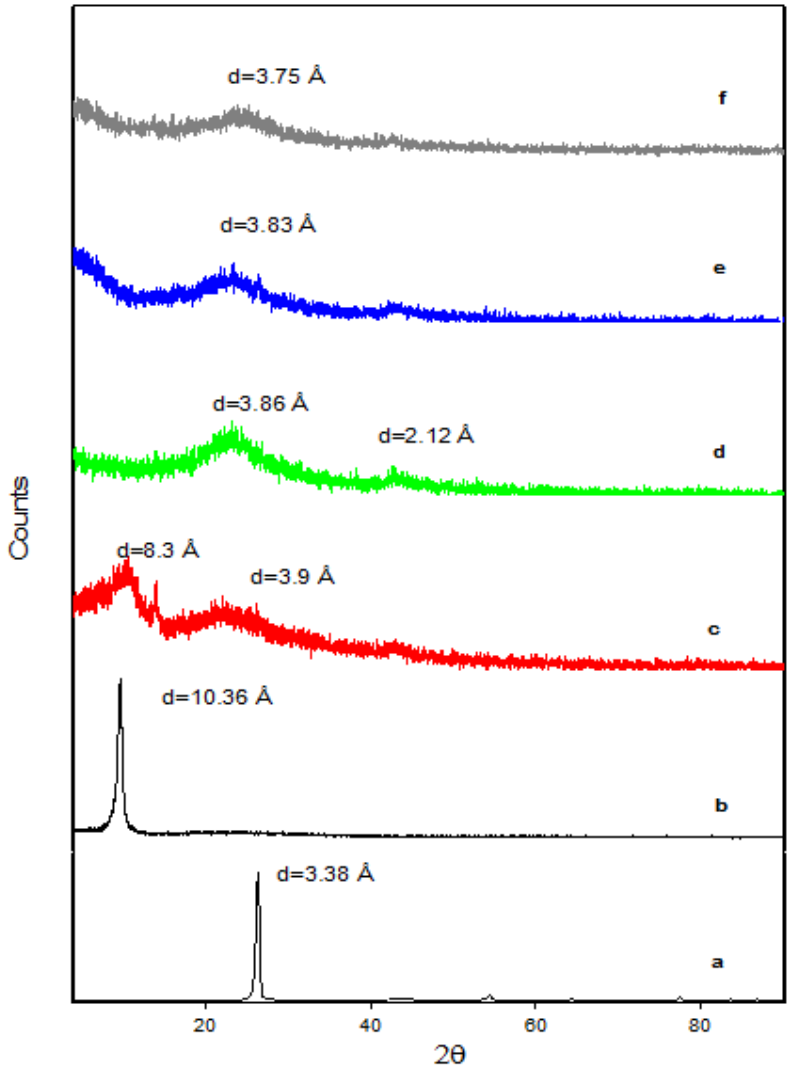

Fig. 2: XRD pattern of Graphite (a) - GO (b) - RRGOs prepared at different absorbed doses of 20 (c) 40(d) and 80 KGy (e) compared to CRGO (f).

Structural changes in GO during γ-irradiation were further investigated by Raman spectroscopy. As shown in Fig. (3), Raman spectra for GO shows two characteristic bands; first is D band at 1350 cm^{-1} refers to the presence of sp^3 defects, edge planes and disordered structures. The second one is G band at 1580 cm^{-1}, corresponding to first-order scattering of the E_{2g} mode for sp^2 domains (Ferrari *et al.,* 2006). Raman spectra for RRGOs and CRGO also contain G and D bands, but the D band was red-shifted to 1340 cm^{-1}.

The degree of order across graphitic plans of sample scan can be indicated by The Tuinstra–Koenig relation (Tuinstra *et al.,* 1970) which is the ratio of the intensity of D band to G band (ID/IG).As presented in Fig (3) and compared to GO, ID/IG of the RRGOs was gradually increased with an increase in the dose up to 1.25 at 80KGy; this increase was higher than that of the CRGO.

This demonstrates that γ- irradiation process in alcohol/water alters the structure of GO with massive defects (In *et al.,* 2010), which can be interpreted by the greater formation of new smaller sp^2-hybridized domains during irradiation (Stankovich *et al.,* 2007).

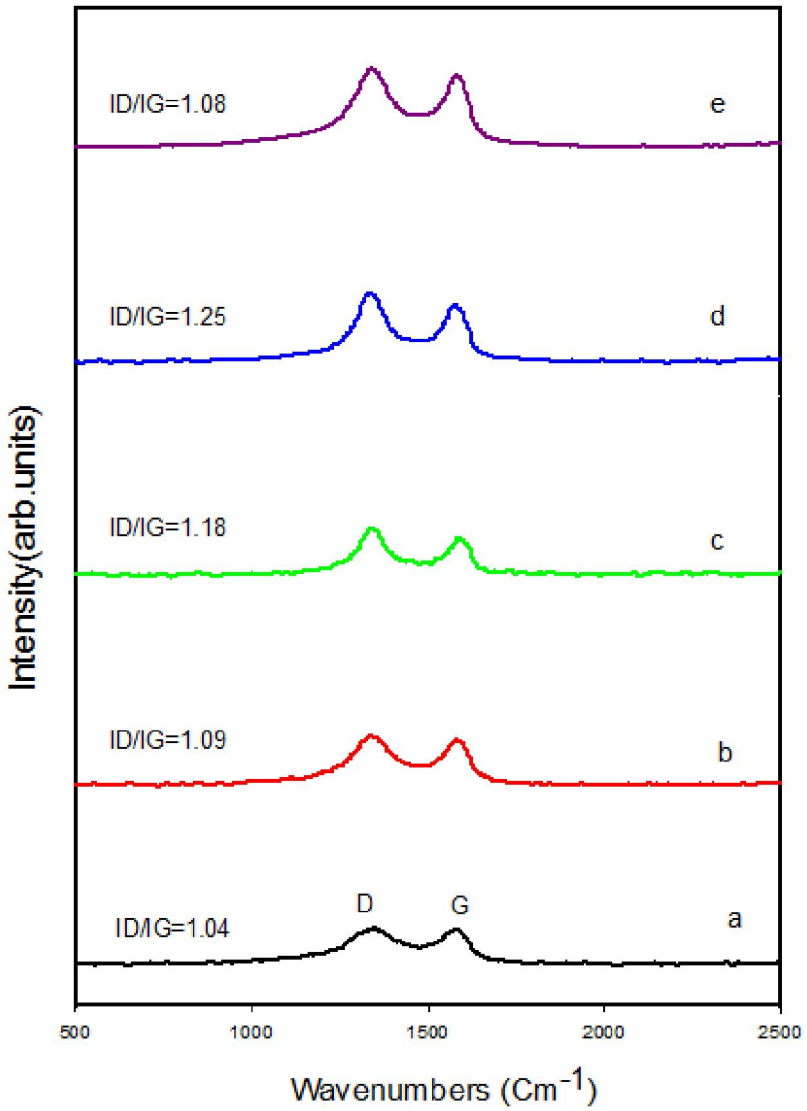

Fig. 3: Raman spectra for GO (a) and RRGOs prepared at different absorbed doses of 20 (b) 40(c) and 80 KGy (d) compared to CRGO (e)

The morphology of GO, RRGOs, and CRGO was studied by TEM. GO has smooth and flat sheets as shown in the figure 4 (a) (Guoxiu *et al.,* 2009). For RRGOs, wrinkles in GO sheets were observed upon irradiation by 20 KGy as shown in figure 4 (b). RRGO prepared at 80 KGy showed a typical crumpled morphology very similar to that of CRGO as shown in figure 4 (c, d), respectively. These topological defects in the RRGOs and CRGO resulted from the multiplicity of chemical carbon bonding in a single carbon layer or a few carbon layers generated during irradiation and chemical reduction (Peng *et al.,* 2011).

Table (1) illustrates the calculated electrical conductivity (σ) for GO, CRGO and RRGOs prepared at different absorbed dose. The poor conductivity of GO could be manifested by its lack of an extended π-conjugated orbital system. The electrical conductivity of RRGOs was increased by an increase in absorbed dose to approximate values at 40 and 80KGy. The increasing conductivity value

of RRGOs compared to GO ascribed to the restoring of the conjugated sp^2-hybridized carbon during irradiation reduction (Dayanand *et al.,* 2013). The slightly higher conductivity of CRGO compared to RRGOs, could be due to increased reduction level of CRGO confirmed previously by XRD as well as increased defects level in RRGOs as illustrated previously by Raman spectra, where defects act as scattering sites and constrain charge transport by limiting the electron mean free path and decreasing conductivity (Hwang *et al.,* 2007).

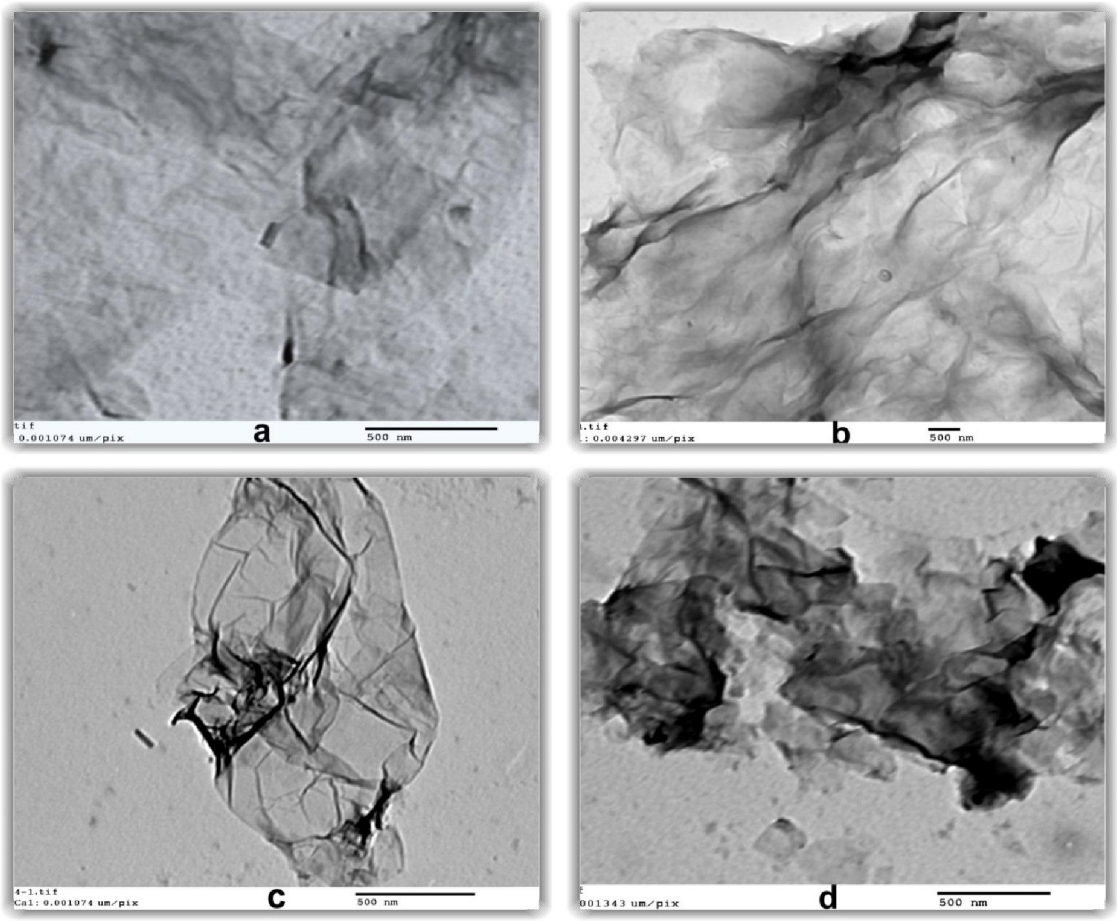

Fig. 4: TEM of GO (a) and RRGOs prepared absorbed doses of 20 (b) and 80 KGy (c) compared to CRGO (d)

Table 1: Calculated electrical conductivity for different samples

Sample	Conductivity (S/m)
GO	5.04E-05
RRGO-20KGy	1.59E-03
RRGO-40KGy	1.68E-01
RRGO-80 KGy	1.75E-01
CRGO	1.92E-01

The TGA curves of Graphite, GO, CRGO and RRGOs prepared at different absorbed dose are given in Figure (3.5). TGA curve of Graphite shows a single major mass loss at 600 ^{o}C due to the pyrolysis of the carbon skeleton (Neil *et al.,* 2009).

The TGA curve of GO shows four distinct temperature spans. First one from ambient temperature to ~150°C (20%) ,where the weight loss is due to loosely bounded or adsorbed water and gas molecules; the second one 150 – 250 °C (~23%) is caused by the decomposition of labile oxygen groups (such as carboxylic, anhydride, or lactone groups). The third temperatures span 250-550 °C (~20%), due to the presence of more thermally-stable oxygen functionalities, while fourth one 600-700 ◦C due to the bulk pyrolysis of the carbon skeleton (Jeong *et al.,* 2009).

On the other hand, TGA curves of RRGOs show that the two main temperature spans 150-250 and 250-550 ◦C dropped more slowly with an increase in the absorbed dose. Moreover, it can be confirmed that the RRGOs prepared at 40 and 80 KGy have more thermal stability than CRGO in these temperature spans, indicating a more effective removal of thermally-labile oxygen species by γ-irradiation reduction compared to chemical reduction (Stankovich *et al.,* 2007; Jianfeng *et al.,* 2010); this result is very similar to that previously reported (Chan *et al.,* 2014).

The increased remaining weight of CRRO was greater than RRGOs could be due to slightly increased reduction degree of CRGO noticed previously by XRD.

The thermal stability was additionally confirmed by determining activation energies of the thermal decomposition of samples by applying the Horowitz–Metzger method (Horowitz, 1963) according to the equation:

$$ln\left[ln\left(\frac{m_o-m_f}{m-m_f}\right)\right]=\frac{E_{a\theta}}{RT_s^2} \quad \text{.....(2)}$$

Where:

m_0, m, and m_f: the initial mass, mass at time t, final mass, respectively,

E_a: the activation energy, R: gas constant, T_s: the reference temperature, which is at the inflection point of the corresponding TGA curves and $\theta=T-T_s$.

Calculated E_a and T_s were scheduled in a Table (2). It's clear that high activation energy of Graphite dramatically decreased in GO due to weakening the Vander Waals interaction upon oxidation process. The activation energy of RRGOs was increased dependent on irradiation dose to a greater value than CRGO, which also confirm the efficient removal of thermally-labile oxygen groups by γ-irradiation.

Table 2: Calculated activation energy for different samples

Sample	Graphite	GO	RRGO (20 KGy)	RRGO (40 KGy)	RRGO (80 KGy)	CRGO
T_S (K)	953	691	787	859	882	835
Activation energy (KJ mole $^{-1}$)	271.8	3.96	81.8	122.7	129.3	86.9

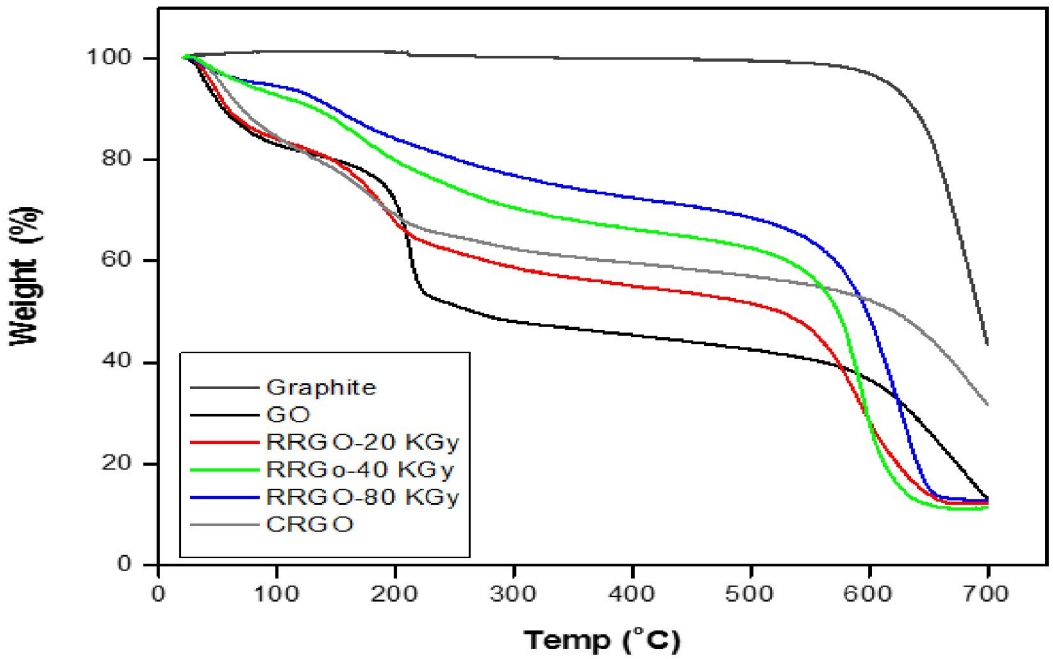

Fig. 5: TGA curves for different samples

Conclusion

GO dissolved in water /ethanol without de-oxygenation has been successfully reduced by γ-irradiation which means oxygen free is not necessary for γ-irradiation reduction as reported earlier (Bowu *et al.,* 2012). FTIR, XRD, and TGA confirmed the reduction process and revealed that the reduction degree was dependent on the absorbed dose. Crumpled morphology of RRGOs and CRGO compared to a smooth morphology of GO also showed by TEM.

Radiation reduction led to increased ratio of defects in RRGOs compared to CRGO which explained by the formation of new smaller sp^2- hybrid domains during irradiation. The electrical conductivity of RRGOs was increased with an increase in absorbed dose up to 0.175 (S/m) compared to 0.192 (S/m) for CRGO. TGA curves show that the thermal stability of RRGOs prepared at 40 and 80 KGy was higher than CRGO in temperature span 150- 550^{o}C corresponding to a higher calculated activation energy, this behavior explained by effective removal of thermally-labile oxygen species during γ - irradiation.

Acknowledgment

I would like to express my deep gratitude to Radiation Physics Department, National Center for Radiation Researches and Technology (NCRRT), Egyptian Atomic Energy Authority (EAEA), for supplying the materials employed and providing facilities.

References

Alfonso, R., J. Xiaoting, H. John *et al.,* 2009. Large area few-layer Graphene films on arbitrary substrates by chemical vapor deposition. Nano Lett, 9(1): 30.

Bowu, Z., L. Linfan, W. Ziqiang *et al.,* 2012. Radiation induced reduction: an effective and clean route to synthesize functionalized graphene. Mater Chem, 22:7775.

Buchsteiner, A., A .Lerf, J .Pieper, 2006. Water dynamics in graphite oxide investigated with neutron scattering. J Phys Chem, 110 (45):22328.

Chan, H. J., W. P. Yong, H .In -Tae *et al.,* 2014. Eco-friendly and simple radiation-based preparation of graphene and its application to organic solar cells. J Phys D: Appl Phys, 47: 015105.

Chen, D., L.Li, L. Guo, 2011. An environment-friendly preparation of reduced graphene oxide nanosheets via amino acid. Nanotechnology, 22(32):325601.

Choi, E.Y., H. H .Tae, H.J. Jihyun *et al.,* 2010. Noncovalent functionalization of graphene with end-functional polymers. J Mater Chem, 20 (10): 1907.

Daniela, C. M., V. K. Dmitry, M. B. Jacob *et al.,* 2010. Improved synthesis of graphene oxide. ACs Nano, 4 (8): 4806.

Dayanand, S., S.Gulbagh, B. Divakar *et al.,* 2013.Electronic structure of graphene oxide and reduced graphene oxide monolayers. Appl Phys Lett, 101 (112).

Ding, Y., P .Zhang, Q. Zhuo *et al.,* 2011. A green approach to the synthesis of reduced graphene oxide nanosheets under UV irradiation. Nanotechnology, 22**:** 215601.

Donghai ,W., C. Daiwon , L. Juan *et al.,* 2009. Self-assembled TiO_2-graphene hybrid nanostructures for enhanced Li ion insertion. ACS Nano, 3 (4):907.

Dongxing, Y., V. Aruna, B. Gulay *et al.,* 2009. Chemical analysis of graphene oxide films after heat and chemical treatments by X-ray photoelectron and Micro-Raman spectroscopy. Carbon, 47(1): 145.

Ferrari, A. C., J. C. Meyer, V. Scardaci *et al.,* 2006. Raman spectrum of graphene and graphene layers. Phys Rev Lett, 97:187401.

Guoxiu, W., S. Xiaoping Y. Jane *et al.,* 2009. Graphene nanosheets for enhanced lithium storage in lithium ion batteries. Carbon, 47:68.

Hailiang, W., T. Joshua, L. Xiaolin *et al.,* 2009. Solvothermal Reduction of Chemically Exfoliated Graphene Sheets. Ame Chem Soc, 131(29):9910.

Helen, W. R., 1998. Radiation Chemistry: Principles and Applications. Ame Chem Soc, 5–33.

Horowitz, H.H . and G.A. Metzger,1963. New analysis of thermogravimetric traces. Anal Chem, 1963, 35:1464.

Hsu, C. L., C. T. Lin, J. H. Huang *et al.,* 2012. Layer-by-Layer Graphene/ TCNQ Stacked Films as Conducting Anodes for Organic Solar Cells. ACS Nano, 6 (6):5031.

Hwang, E.H., S. Adam and S. D .Sarma, 2007. Carrier transport in two-dimensional graphene layers. Phys Rev Lett, 98:186806.

In, K. M., L. Junghyun, S. Rodney *et al.,* 2010. Reduced graphene oxide by chemical graphitization. Nat Commun, 1(6):73.

Jeong, H. K., M. H. Jin, K. P. So *et al.,* 2009. Tailoring the characteristics of graphite oxides by different oxidation times. J Phys D: Appl Phys, 42(6).

Jianfeng,S., H. Yizhe, S. Min et al,2010. One step synthesis of graphene oxide-magnetic nanoparticle composite, J Phys Chem C, 114(3):1498.

Junbo, W., A. Mukul, A. B. Héctor *et al.,* 2010. Organic light-emitting diodes on solution-processed graphene transparent electrodes. ACS Nano, 4 (1): 43.

Leila, S. and A. Anjali, 2015. Synthesis of graphene using gamma radiations. Bull Mater Sci, 38: 739.

Meryl, D. S., P. Sungjin, Z .Yanwu *et al.,* 2008. Graphene -based ultracapacitors. Nano Lett, 8: 3498.

Neil, W., A. P. Priyanka, B. Richard *et al.,* 2009. Graphene oxide: structural analysis and application as a highly transparent support for electron microscopy. ACS Nano, 3(9): 2547.

Peng, S., Z .Xiaoyan, S .Mingxuan *et al.,* 2011. Synthesis of graphene nanosheets via oxalic acid-induced chemical reduction of exfoliated graphite oxide. RSC Adv, 2(3): 1168.

Stankovich, S., D.A. Dikin, R. Piner *et al.,* 2007. Synthesis of graphene-based nanosheets via chemical reduction of exfoliated graphite oxide. Carbon, 45(7): 1558.

Tuinstra, F. and J. L .Koenig, 1970. Raman spectrum of graphite. Chem Phys, 53: 1126.

Walt, A. H., B, Claire, W. Xiaosong *et al.,* 2007.Epitaxial graphene. Sol Stat Commun, 143: 92.

Xiangbo, M., G. Dongsheng, L. Jian et al, 2010. Non-aqueous approach to synthesize amorphous/crystalline metal oxide –graphene nanosheets hybride composites. J Phys Chem C, 114:18330.

Xuan, W., Z. Linjie, T. Nok *et al.,* 2008. Transparent Carbon films as electrode in organic solar cells. Angewandte Chemie Int. 47(16): 2990.

Yuanbo, Z., P. S. Joshua, V. P. William *et al.,* 2005.Fabrication and electric-field-dependent transport measurements of mesoscopic graphite devices. Appl Phys Lett, 86:073104.

Yuyan,S., W. Jun, E. Mark *et al.,* 2010. Facile and controllable electrochemical reduction of graphene oxide and its application. J Mate Chem, 20:743.

Zhiwei, X., H.Yudong, M. Chunying et al., 2010. Effect of gamma-ray radiation on the polyacrylonitrile based Carbon fibers. Rad Phys and Chem., 79(8):839